

1 **TITLE:**

2 Nano-thermal imaging of the stratum corneum and its potential use for understanding of  
3 the mechanism of skin penetration enhancer

4  
5 **AUTHOR NAMES:**

6 Choon Fu Goh \* † ‡, Jonathan G Moffat §, Duncan Q M Craig †, Jonathan Hadgraft †,  
7 Majella E. Lane †

8  
9 **AUTHOR ADDRESS:**

10 † Department of Pharmaceutical Technology, School of Pharmaceutical Sciences,  
11 Universiti Sains Malaysia, Penang 11800, Malaysia

12 ‡ Department of Pharmaceutics, UCL School of Pharmacy, 29-39 Brunswick Square,  
13 London WC1N 1AX United Kingdom

14 § Asylum Research an Oxford Instruments Company, Halifax Road, High Wycombe,  
15 Buckinghamshire, HP12 3SE United Kingdom

16 \* Corresponding author: Department of Pharmaceutical Technology, School of  
17 Pharmaceutical Sciences, Universiti Sains Malaysia, Penang 11800, Malaysia. Tel:  
18 +604-6532074. Fax: +604-6570017. Email: gohchoonfu@hotmail.com

19  
20

21 **ABSTRACT:**

22 Nano-thermal analysis (nano-TA) is a localised thermal technique which maps a surface  
23 in terms of thermal transitions by combining atomic force microscopy with the use of  
24 thermal probes, allowing a spatial resolution of sub-100nm. In this communication, we  
25 describe the application of a localised nano-TA approach, transition temperature  
26 microscopy (TTM), to investigate the thermotropic properties of porcine SC (PSC) as a  
27 function of depth and the influence of penetration enhancer on the nano-thermal  
28 properties of PSC. The investigations were conducted on PSC removed using tape  
29 strips. The transition temperature of PSC recorded at ~220°C was ascribed to protein  
30 denaturation/degradation. A decrease in the transition temperature was observed with  
31 an increase of skin depth. 'Transition depression' was observed when PSC was treated  
32 with propylene glycol, suggesting its water extraction effect on SC protein and a drop in  
33 the biomechanical properties of the SC. TTM has the potential to be extended to on *in*  
34 *situ* investigations of various penetration enhancers.

35

36 **KEYWORDS:**

37 Nano-TA; stratum corneum; protein denaturation/degradation; porcine skin; skin  
38 penetration enhancer

39

40 **ABBREVIATIONS:**

41 AFM: Atomic force microscopy

42 HSC: Human stratum corneum

43 LTA: Localised thermal analysis  
44 Nano-TA: Nano-thermal analysis  
45 PG: Propylene glycol  
46 PSC: Porcine stratum corneum  
47 SC: Stratum corneum  
48 TTM: Transition temperature microscopy

49

50 **MANUSCRIPT BODY:**

51 Advances in the field of nanotechnology and instrumentation in recent years have  
52 opened up new opportunities to probe drug delivery at the molecular level. As an  
53 extension of localised thermal analysis (LTA), nano-thermal analysis (nano-TA) has  
54 gained popularity in pharmaceutical research as a physical characterisation tool for solid  
55 dosage forms. By employing a thermal probe in a scanning probe microscope, spatially  
56 resolved localised measurements on the surface of a sample is achieved using nano-TA  
57 (1). The nano-machined probes measure a thermal event via penetration of the probe  
58 into the sample because of surface softening upon heating. Unlike bulk thermal  
59 analysis, nano-TA provides spatially resolved information about the surface properties  
60 of materials. The technique has been used to differentiate various materials including  
61 amorphous and crystalline forms, to map samples with high spatial resolution and to  
62 provide 3D information (2). Transition temperature microscopy (TTM) applies the same  
63 principles of nano-TA but measurements are carried out in a grid pattern (1). This

64 creates a TTM image with each pixel referring to a transition temperature assigned  
65 using a colour palette. TTM was first used to map the surface of  
66 paracetamol/hydroxypropyl methylcellulose (HPMC) compacts and to determine  
67 distribution of materials (1). TTM provided insight into the phase separation in  
68 nilvadipine/HPMC spray dried particles at different nitrogen flow rates (3), fentanyl-  
69 poly(vinylpyrrolidone) (PVP) solid dispersion thin films under high humidity (4) and  
70 cyclosporine A-Eudragit E PO hot melt extruded dispersions prepared at different  
71 mixing temperatures (5). It has also been used to characterise PVP nanofibers to  
72 identify the materials (6). The application of TTM in characterising the solid drug  
73 products has been shown to be a very promising approach to understand the  
74 distribution of different materials on the surface. This technique shows advantages over  
75 basic atomic force microscopy (AFM) by providing thermal information of the sample  
76 apart from the topographical images. The identification of different materials present in a  
77 sample renders difficult in AFM images.

78 To date, the thermal behaviour of the stratum corneum (SC) has been studied using  
79 bulk thermal analysis, namely differential scanning calorimetry. This method, however,  
80 provides only global information on the overall thermotropic properties of the SC. The  
81 advent of nano-characterisation methods such as TTM is the major motivation for the  
82 present investigation in order to understand the thermal properties of the SC at the  
83 nano-scale with high spatial resolution.

84 Penetration enhancers have been extensively used in topical and transdermal drug  
85 delivery to accelerate the transport of drug molecules into the skin (7). However, the  
86 underlying mechanisms of most penetration enhancers have not been fully understood.

87 Therefore, it is also of interest to explore the potential of TTM to provide more  
88 information regarding to the possible enhancement mechanism of penetration enhancer  
89 in improving transport of drug molecules into the skin.

90 TTM is a highly sensitive tool which works best for samples with a consistent thickness  
91 or a flat surface. The normal skin surface, however, is rough and uneven and is not  
92 suitable for direct contact with TTM probes as it may damage thermal probes. Therefore,  
93 the SC was collected by tape stripping for this work.

94 Porcine ear skin was used as it is an accepted surrogate model for human skin. Fresh  
95 porcine ears were obtained from a local abattoir and washed carefully with deionised  
96 water. The outer skin membrane was carefully isolated from the underlying tissues and  
97 the hair was trimmed carefully using scissors. The prepared skin was stored at -20°C  
98 and thawed at room temperature before use. The skin was mounted in Franz-type  
99 diffusion cells (diffusional area =  $\sim 1 \text{ cm}^2$ ) at  $32 \pm 0.5^\circ\text{C}$  with and without application of  
100 PG ( $2 \mu\text{l}/\text{cm}^2$ ) for 24 h. The receptor phase was filled with phosphate buffer saline (pH  
101  $7.3 \pm 0.2$ ). After 24 h, *in vitro* tape stripping with porcine ear skin was carried out as  
102 reported by Klang, Schwarz (8) (9). Excess PG was removed gently using dry tissues  
103 before tape stripping. A total of 20 sequential D-Squame<sup>®</sup> tapes were obtained for the  
104 tape stripping procedure. This *in vitro* tape stripping procedure was standardised in  
105 terms of intensity with a pressure applicator and duration of pressure application (5 s)  
106 as well as the speed of tape stripping to ensure reproducibility of the measurements.  
107 The amount of SC protein collected on each tape strip was quantified with an infrared  
108 (IR) densitometer SquameScan<sup>®</sup> 850A at a wavelength of 850 nm (Heiland Electronic  
109 GmbH, Wetzlar, Germany) based on the absorption values obtained from IR

110 densitometry – absorption (%) = 0.41 x mass of protein ( $\mu\text{g}/\text{cm}^2$ ) (8). From the  
111 measured area that was tape stripped area, the SC thickness, which reflects the depth  
112 of the SC barrier may be calculated using a SC density of  $1 \text{ g}/\text{cm}^3$ . (8,10)

113 TTM measurements were conducted using a VESTA<sup>®</sup> Nano Thermal Analyser (Anasys  
114 Instruments Corp., Santa Barbara, CA, US) with a nano-TA probe (Bruker AXS S.A.S,  
115 Marne la Vallee Cedex 2, France) as described elsewhere (5). The device was  
116 connected to a nanoTA2 controller (Anasys Instruments Corp., Santa Barbara, CA, US)  
117 for voltage adjustment to the tip. The cantilever deflection is monitored by the sensor  
118 signal (V). Temperature calibration was carried out for the probe using the  
119 manufacturer-supplied melting point standards – polycaprolactone ( $55^\circ\text{C}$ ), polyethylene  
120 ( $116^\circ\text{C}$ ) and polyethylene terephthalate ( $235^\circ\text{C}$ ). The softening of the materials caused  
121 by the penetration of the probe into the surface with heat was determined as a thermal  
122 event. Samples were firmly attached to a magnetic stud using double-sided tape before  
123 mounting on an X-Y translation microscope stage. TTM imaging was performed based  
124 on thermal transition temperatures in LTA. An underlying heating rate of  $10^\circ\text{C}/\text{s}$  was  
125 applied in LTA from room temperature ( $25^\circ\text{C}$ ) to  $250^\circ\text{C}$ , with a cooling rate of  $100^\circ\text{C}/\text{s}$   
126 and a data rate of 20 point/s. An area of interest ( $30 \times 30 \mu\text{m}$  or  $10 \times 10 \mu\text{m}$ ) on a  
127 sample surface was identified and an optical microscope was used to capture the image  
128 of the sample surface. The TTM image was constructed based on a particular colour  
129 palette where a colour was assigned to each transition temperature detected. The  
130 resolution of the TTM image was set at  $1 \times 1 \mu\text{m}$  and the distance between locations for  
131 measurement was fixed at  $1 \mu\text{m}$ .

132 The mass of protein removed by sequential tape stripping is shown Figure 1. The  
133 amount of protein removed progressively decreased with the number of tape strips.  
134 Similar observations have been reported by Klang, Schwarz (8) using the same tapes  
135 (D-Squame<sup>®</sup>). A study comparing *in vitro* and *in vivo* tape stripping on human skin also  
136 confirmed a similar pattern using the same tapes (10). The cumulative thickness of the  
137 SC removed increases with the number of tape strip. The calculated SC thickness was  
138  $6.6 \pm 0.8 \mu\text{m}$  but this does not represent the actual thickness of the SC because the 20  
139 sequential tape strips does not remove the entire SC.

140 TTM images of the first and second tape strips are illustrated in Figure 2. Two domains  
141 (red/yellow and purple colours) with transition temperatures of  $\sim 220^\circ\text{C}$  and  $25^\circ\text{C}$  were  
142 identified in both images. The transition temperature of  $\sim 220^\circ\text{C}$  within the red domain  
143 refers to the SC. The first two tape strips were scanned with an area of  $30 \times 30 \mu\text{m}$  in  
144 order to elucidate the differences between the SC (red domain) and the tape adhesive  
145 (purple domain). The detection of the transition temperature around  $220^\circ\text{C}$  for the SC is  
146 largely related to protein denaturation and degradation. Bulk thermal analysis of PSC  
147 using differential scanning calorimetry (DSC) has confirmed that at about  $90^\circ\text{C}$  there is  
148 generally an irreversible SC protein denaturation (11-16). Bulgon and Vinson (17)  
149 suggested that denaturation of keratin in human stratum corneum (HSC) may contribute  
150 to the transition temperature above  $180^\circ\text{C}$ . The transition temperature of PSC reported  
151 in this study is also similar to the highest transition temperature determined using  
152 thermomechanical analysis of HSC (18,19). This is generally correlated with the thermal  
153 decomposition of skin tissue and was confirmed by DSC and visual observation (20).  
154 Recent work studying the effects of heat on human skin indicated that the SC started to

155 decompose when it was heated from 150 – 200°C (21). Epidermal tissue changes under  
156 the influence of heat are complex. The increase of tension of the epidermis upon  
157 heating may be attributed to the disruption of the  $\alpha$ -helix and the build-up of  $\beta$  keratin  
158 (22). When heat is applied to the SC,  $\alpha$ -keratin is converted to the  $\beta$  form because of  
159 fractures in cross-linkages of keratin filaments (15).

160 The anisotropic structure of SC is greatly influenced by the organisation of keratin.  
161 Because of the heterogeneous distribution of keratin filaments, the effect of temperature  
162 on viscoelastic properties of SC will vary from one tape strip to the next. Comparisons of  
163 all 20 tape strips were carried out using a scanning area of 10 × 10  $\mu\text{m}$  on the SC and  
164 excluding the tape adhesive (Figure 3).

165 Figure 4A shows the correlation of the transition temperature and protein mass  
166 collected on each strip. Protein mass extracted indicates the thickness of the SC  
167 sample. The transition temperature of PSC decreases gradually with the number of tape  
168 strips removed. The mean transition temperature between each layer of tape strips are  
169 statistically significant differences (ANOVA,  $p < 0.05$ ). In addition, it is interesting to note  
170 that the higher amount of SC protein/keratin (or the thicker of the SC extracted) resulted  
171 in a higher transition temperature (Figure 4A). The relationship between the mean  
172 transition temperature and protein mass is shown clearly in Figure 4B. Heat is required  
173 to break the cross linking of keratin filaments in the SC, converting the  $\alpha$ -keratin to the  $\beta$   
174 form (15). Substantial energy is required for transforming  $\alpha$ -keratin to the  $\beta$  form in tape  
175 strips containing more keratin. An increase in the  $\beta/\alpha$  ratio with heating was observed by  
176 Lin and co-workers indicating a continuous conversion of these structures (15). It may  
177 happen similarly in this work where a high degree of keratin denaturation in a thick SC



178 sample (high protein mass) may result in a late penetration of the nano-TA probe into  
179 the SC. Thus, this causes a higher transition temperature.

180 The correlation between the transition temperature and protein mass may be further  
181 understood using the variations in the colour assigned (red to yellow) for PSC for  
182 distribution of keratin content. In this case, the red colour refers to a higher level of  
183 keratin filaments, resulting in a higher transition temperature. This may reflect a late  
184 penetration of the probe into the SC (penetration at a higher transition temperature)  
185 because more energy in the form of heat is needed to break the cross linking of the  
186 keratin filaments. The yellow region is assigned to an area with less keratin filaments,  
187 showing an early penetration temperature of the probe. A recent approach using AFM  
188 with a tunable IR laser source (AFM-IR) showed that the variation of the intensities of  
189 absorption peak at  $3290\text{ cm}^{-1}$  (mostly due to the N–H stretching vibration of amide A in  
190 the keratin) in the HSC sample is related to the total protein content at the point of  
191 measurement (23). A weaker band at  $3290\text{ cm}^{-1}$  was linked to a lower total protein  
192 content relative to the hydrophobic lipid-like compounds. This observation supports the  
193 appearance of two different colours (red/yellow) within the same domain assigned to the  
194 PSC in this study. The colour variation in the PSC, therefore, reflects different amounts  
195 of protein (keratin) or different thickness of the SC sample at the scanning point as  
196 explained above.

197 PG is a commonly used glycol in topical formulations especially for improving the  
198 transport of poorly soluble materials into the skin. Thermal analysis of the effect of PG  
199 on skin has demonstrated the possibility of a dehydrating effect of PG on the SC

200 protein(24). Therefore, PG is shown as a good candidate in this work as TTM data  
201 reported the transition temperature of SC protein instead of the lipids.

202 The SC thickness removed (a total of 20 tape strips) from the skin treated with PG was  
203  $6.6 \pm 0.7 \mu\text{m}$  and there is no statistically significant difference reported in the SC  
204 thickness removed compared with the control study (Mann-Whitney test,  $p > 0.05$ ). The  
205 amount of the removed protein from individual tape strip also showed no statistical  
206 differences (Mann-Whitney test,  $p > 0.05$ ) compared with the control with the exception  
207 of the first tape ( $p < 0.05$ ) (Figure 1). The SC in this first tape has the highest exposure  
208 time to PG before PG evaporates or permeates through the skin. PG has no large  
209 impact on the removal of the SC in the deeper layers. Although PG does not have a  
210 major influence on the protein content removed by tape stripping, it shows a  
211 pronounced effect on the thermal properties of PSC. From the TTM images in Figure 5,  
212 a homogenous yellow/green region was obtained consistently for all selected tapes.  
213 Transition temperatures for this yellow/green zone ranged from 175°C to 190°C as listed  
214 in Table 1, suggesting a significant drop in the transition temperature of PSC as  
215 compared to the same tape reported in the untreated samples (Student's  $t$  test,  $p <$   
216  $0.05$ ). This phenomenon is termed here as 'transition depression'.

217 Previous DSC studies which investigated the change of thermal behaviour after  
218 treatment with PG revealed the absence of the protein denaturation endotherm (24).  
219 The loss of the protein peak may reflect water extraction from the protein by PG (24,25).  
220 Ostrenga, Steinmetz (26) previously reported that skin pliability was reduced due to the  
221 dehydration effect of PG. The water extraction effect on the SC protein could be related  
222 to the transition depression observed for the SC in the presence of PG. Dehydration of

223 the SC protein could change the biomechanical properties of the SC (27). The SC  
224 plasticised with water has a high stretching capacity which requires more energy to  
225 weaken the biomechanical properties of the SC (27). In less hydrated SC,  
226 biomechanical strength withstanding the tension applied without fracture is far weaker  
227 than that of hydrated SC. It may be hypothesised that water extraction from the protein  
228 content by PG has weakened the biomechanical properties of PSC in the same way.  
229 Loss of water has impaired the integrity of SC to resist force applied by the heated  
230 probe. Consequently, the cantilever of the probe deflected to a smaller extent, giving  
231 rise to an early penetration of the probe into the SC. The greatest reduction of transition  
232 temperature was reported in the first few layers (Table 1). This may be due to the  
233 highest contact time of these SC layers with PG before PG depleted from the skin.  
234 Under these circumstances, water extraction by PG is more substantial in the upper  
235 layer of the SC, further weakening the mechanical strength of SC. This modification of  
236 the biomechanical properties of SC associated with the use of PG has not been  
237 reported previously using other thermal analyses.

238 In summary, we demonstrated that TTM is a powerful nano-thermal technique in  
239 describing the thermal properties of PSC *in situ* at a high spatial resolution. TTM is able  
240 to characterise the thermal properties of the SC as a function of depth which is  
241 impossible to be achieved by using a conventional thermal analysis such as DSC. Also,  
242 the thermal measurement using TTM can be conducted at ambient environment which  
243 mimics the actual condition. This technique is convenient to use and does not require  
244 any other accessories such as pan and purging gas. By having these advantages, we  
245 managed to show that the influence of PG on the local thermal and biomechanical

246 properties of the SC can be reflected by the changes of the transition temperature.  
247 Therefore, we believe that this technique could be adapted to further evaluate the  
248 underlying mechanism of various skin penetration enhancers which have been  
249 previously reported to have interaction with SC protein and ability to modify the protein  
250 conformation such as dimethyl sulphoxide (7). However, the application of TTM is  
251 limited to the changes occurred to solid objects such as protein. The observation  
252 involving liquid such as SC lipid is not suitable by using TTM. Techniques such as DSC  
253 and ATR-FTIR spectroscopy may be used to support the action of skin penetration  
254 enhancers on the SC lipid.

255

#### 256 **ACKNOWLEDGEMENT:**

257 The authors would like to thank Ministry of Education Malaysia for PhD funding of  
258 Choon Fu Goh.

259

#### 260 **REFERENCES:**

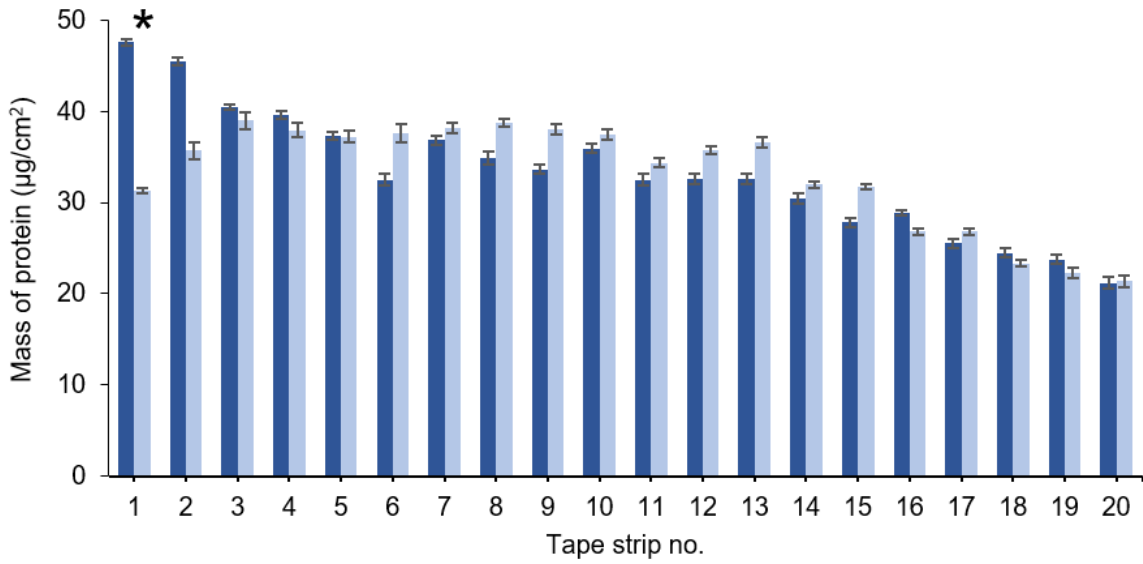
- 261 1. Dai X, Moffat JG, Wood J, Reading M. Thermal scanning probe microscopy in  
262 the development of pharmaceuticals. *Advanced Drug Delivery Reviews*.  
263 2012;64(5):449-60.
- 264 2. Zhang J, Bunker M, Chen X, Parker AP, Patel N, Roberts CJ. Nanoscale thermal  
265 analysis of pharmaceutical solid dispersions. *International Journal of Pharmaceutics*.  
266 2009;380(1–2):170-3.
- 267 3. Kojima Y, Ohta T, Shiraki K, Takano R, Maeda H, Ogawa Y. Effects of spray  
268 drying process parameters on the solubility behavior and physical stability of solid  
269 dispersions prepared using a laboratory-scale spray dryer. *Drug Development and*  
270 *Industrial Pharmacy*. 2012;39(9):1484-93.

- 271 4. Qi S, Moffat JG, Yang Z. Early stage phase separation in pharmaceutical solid  
272 dispersion thin films under high humidity: Improved spatial understanding using probe-  
273 based thermal and spectroscopic nanocharacterization methods. *Molecular*  
274 *Pharmaceutics*. 2013;10(3):918-30.
- 275 5. Moffat J, Qi S, Craig DM. Spatial characterization of hot melt extruded dispersion  
276 systems using thermal atomic force microscopy methods: The effects of processing  
277 parameters on phase separation. *Pharmaceutical Research*. 2014;31(7):1744-52.
- 278 6. Raimi-Abraham BT, Mahalingam S, Edirisinghe M, Craig DQM. Generation of  
279 poly(N-vinylpyrrolidone) nanofibres using pressurised gyration. *Materials Science and*  
280 *Engineering: C*. 2014;39:168-76.
- 281 7. Lane ME. Skin penetration enhancers. *International Journal of Pharmaceutics*.  
282 2013;447(1–2):12-21.
- 283 8. Klang V, Schwarz JC, Hartl A, Valenta C. Facilitating *in vitro* tape stripping:  
284 Application of infrared densitometry for quantification of porcine stratum corneum  
285 proteins. *Skin Pharmacology and Physiology*. 2011;24(5):256-68.
- 286 9. J.C. Schwarz, V. Klang, M. Hoppel, M. Wolzt, C. Valenta, Corneocyte quantification  
287 by NIR densitometry and UV/VIS spectroscopy for human and porcine skin  
288 and the role of skin cleaning procedures, *Skin Pharmacol. Physiol.* 25 (3) (2012)  
289 142–149.
- 290 10. T. Hahn, S. Hansen, D. Neumann, K.H. Kostka, C.M. Lehr, L. Muys, et al., Infrared  
291 densitometry: a fast and non-destructive method for exact stratum corneum depth  
292 calculation for *in vitro* tape-stripping, *Skin Pharmacol. Physiol.* 23 (4) (2010) 183-192.
- 293 11. K. Knutson, R.O. Potts, D.B. Guzek, G.M. Golden, J.E. McKie, W.J. Lambert, et al.,  
294 Macro- and molecular physical-chemical considerations in understanding drug  
295 transport in the stratum corneum, *J. Control. Release* 2 (1985) 67–87.
- 296 12. G.M. Golden, D.B. Guzek, A.E. Kennedy, J.E. McKie, R.O. Potts, Stratum corneum  
297 lipid phase transitions and water barrier properties, *Biochemistry* 26 (8) (1987)  
298 2382–2388.
- 299 13. G.M. Golden, J.E. McKie, R.O. Potts, Role of stratum corneum lipid fluidity in  
300 transdermal drug flux, *J. Pharm. Sci.* 76 (1) (1987) 25–28.
- 301
- 302 14. M. Francoeur, G. Golden, R. Potts, Oleic acid: its effects on stratum corneum in  
303 relation to (trans)dermal drug delivery, *Pharm. Res.* 7 (6) (1990) 621–627.
- 304
- 305 15. S.Y. Lin, K.J. Duan, T.C. Lin, Simultaneous determination of the protein conversion  
306 process in porcine stratum corneum after pretreatment with skin enhancers by a  
307 combined microscopic FT-IR/DSC system, *Spectrochim. Acta Part A* 52 (12) (1996)  
308 1671–1678.
- 309

- 310 16. S.Y. Lin, R.C. Liang, T.C. Lin, Lipid and protein thermotropic transition of porcine  
311 stratum corneum by microscopic calorimetry and infrared spectroscopy, *J. Chin.*  
312 *Chem. Soc.* 41 (4) (1994) 425–429.  
313
- 314 17. J.J. Bulgin, L.J. Vinson, The use of differential thermal analysis to study the bound  
315 water in stratum corneum membranes, *Biochim. Biophys. Acta (BBA)* 136 (3)  
316 (1967) 551–560.  
317
- 318 18. W.T. Humphries, R.H. Wildnauer, Thermomechanical analysis of stratum corneum  
319 i. Technique, *J. Invest. Dermatol.* 57 (1) (1971) 32–37.  
320
- 321 19. W.T. Humphries, R.H. Wildnauer, Thermomechanical analysis of stratum corneum  
322 ii. Application, *J. Invest. Dermatol.* 58 (1) (1972) 9–13.  
323
- 324 20. D.L. Miller, R.H. Wildnauer, Thermoanalytical probes for the analysis of physical  
325 properties of stratum corneum, *J. Invest. Dermatol.* 69 (3) (1977) 287–289.  
326
- 327 21. J.H. Park, J.W. Lee, Y.C. Kim, M.R. Prausnitz, The effect of heat on skin  
328 permeability, *Int. J. Pharm.* 359 (1–2) (2008) 94–103.  
329 [
- 330 22. H.P. Baden, A.M. Gifford, Isometric contraction of epidermis and stratum corneum  
331 with heating, *J. Invest. Dermatol.* 54 (4) (1970) 298–303.  
332
- 333 23. C. Marcott, M. Lo, K. Kjoller, Y. Domanov, G. Balooch, G.S. Luengo, Nanoscale  
334 infrared (IR) spectroscopy and imaging of structural lipids in human stratum  
335 corneum using an atomic force microscope to directly detect absorbed light from a  
336 tunable IR laser source, *Exp. Dermatol.* 22 (6) (2013) 419–421.  
337
- 338 24. J.A. Bouwstra, M.A. de Vries, G.S. Gooris, W. Bras, J. Brussee, M. Ponc, M.  
339 Thermodynamic and structural aspects of the skin barrier, *J. Control. Release* 15 (3)  
340 (1991) 209–219.  
341
- 342 25. J.A. Bouwstra, L.J.C. Peschier, J. Brussee, H.E. Boddé, Effect of n-alkyl-  
343 azocycloheptan- 2-ones including azone on the thermal behaviour of human stratum  
344 corneum, *Int. J. Pharm.* 52 (1) (1989) 47-54.  
345
- 346 26. J. Ostrenga, C. Steinmetz, B. Poulsen, S. Yett, Significance of vehicle composition II:  
347 prediction of optimal vehicle composition, *J. Pharm. Sci.* 60 (8) (1971) 1180-1183.  
348
- 349 27. Wildnauer RH, Bothwell JW, Douglass AB. Stratum corneum biomechanical  
350 properties. I. Influence of relative humidity on normal and extracted human stratum  
351 corneum. *Journal of Investigative Dermatology.* 1971;56(1):72-8.

352

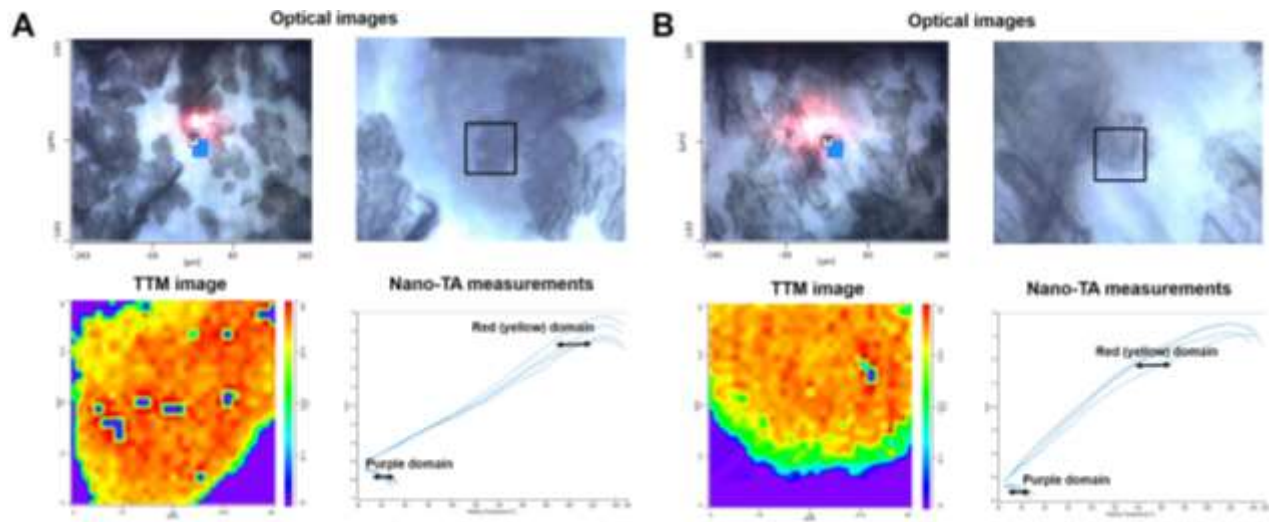
353 **FIGURES:**



354

355 Figure 1 Mass of SC protein removed across the porcine ear skin with 20 tape strips  
356 with (light blue bars) and without (dark blue bars) the application of PG (n = 5, mean ±  
357 SD). \* indicates statistically significant difference (Mann-Whitney test,  $p < 0.05$ ).

358



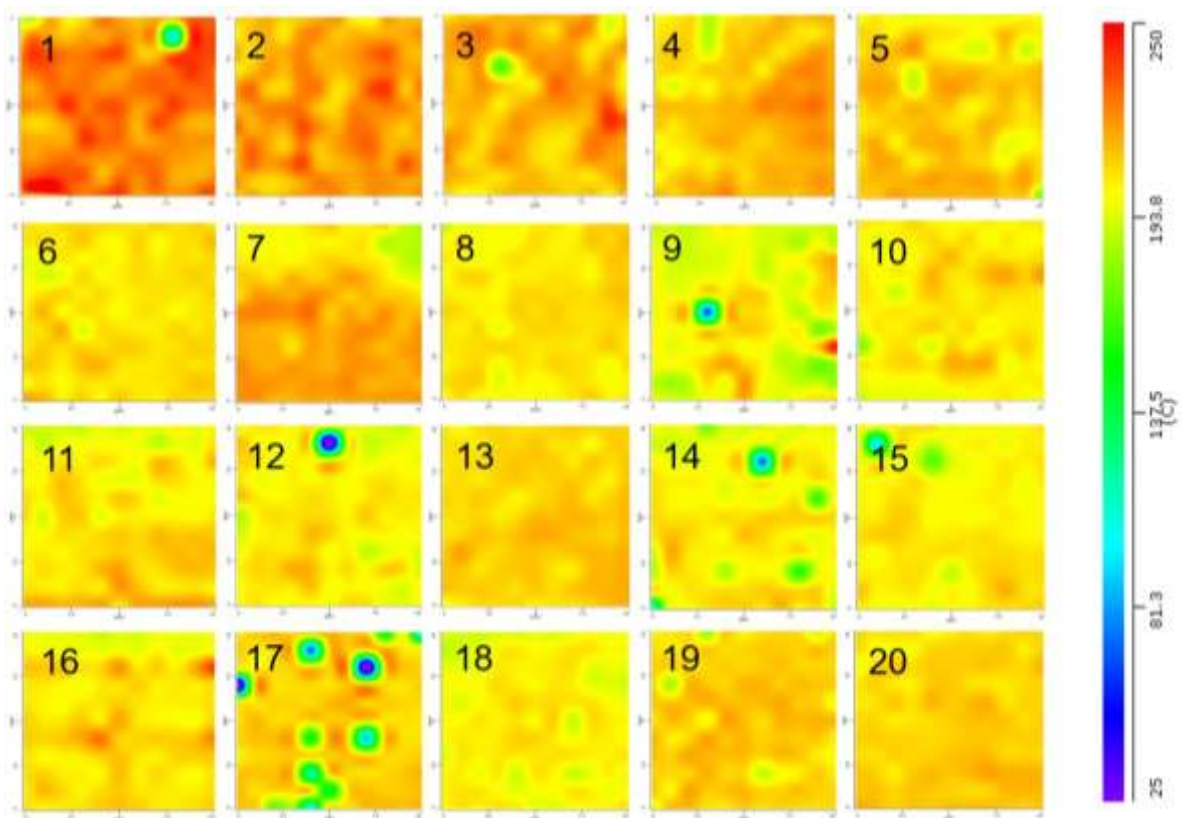
359

360 Figure 2 TTM data for the (A) first and (B) second tape strips of PSC in the control study  
 361 (area:  $30 \times 30 \mu\text{m}$ ; resolution:  $1 \times 1 \mu\text{m}$ )

362

363



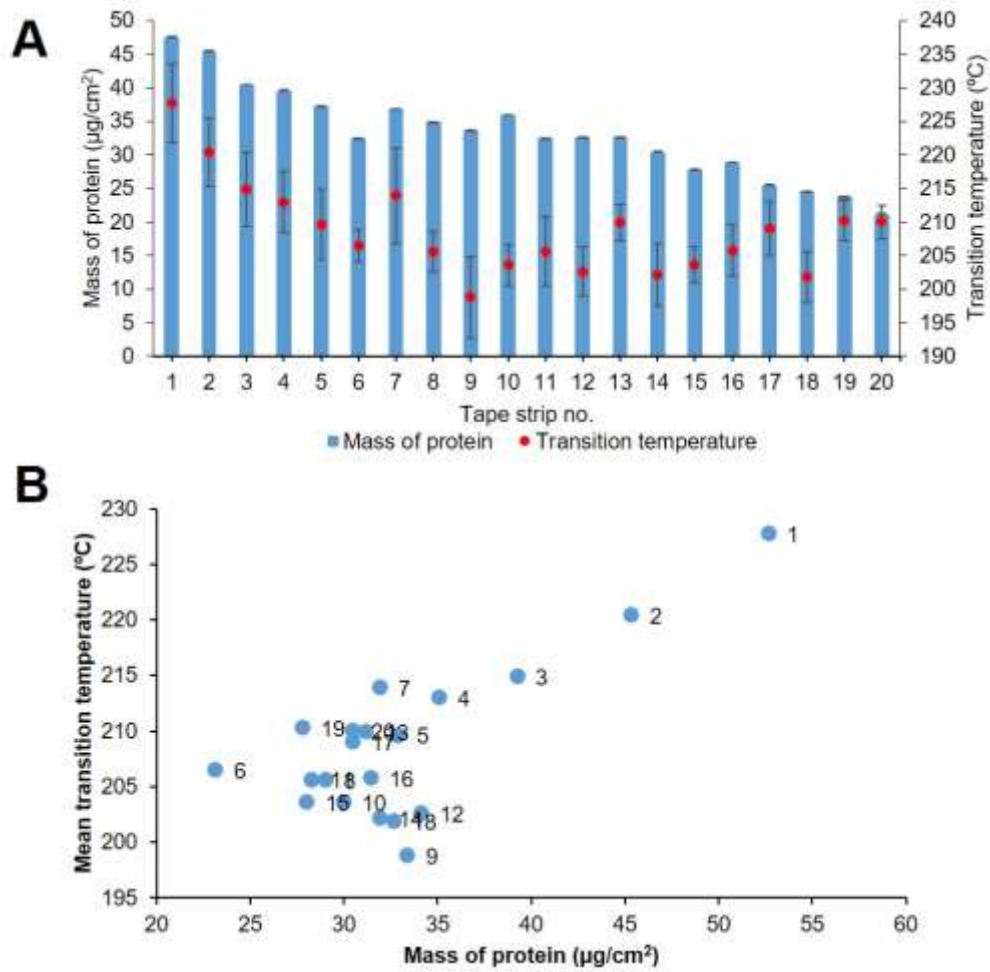


364

365 Figure 3 TTM images for all 20 tape strips of PSC in the control study (Area:  $10 \times 10$   
 366  $\mu\text{m}$ ; Resolution:  $1 \times 1 \mu\text{m}$ ). The number in the TTM images refers to the tape strip  
 367 number.

368

369



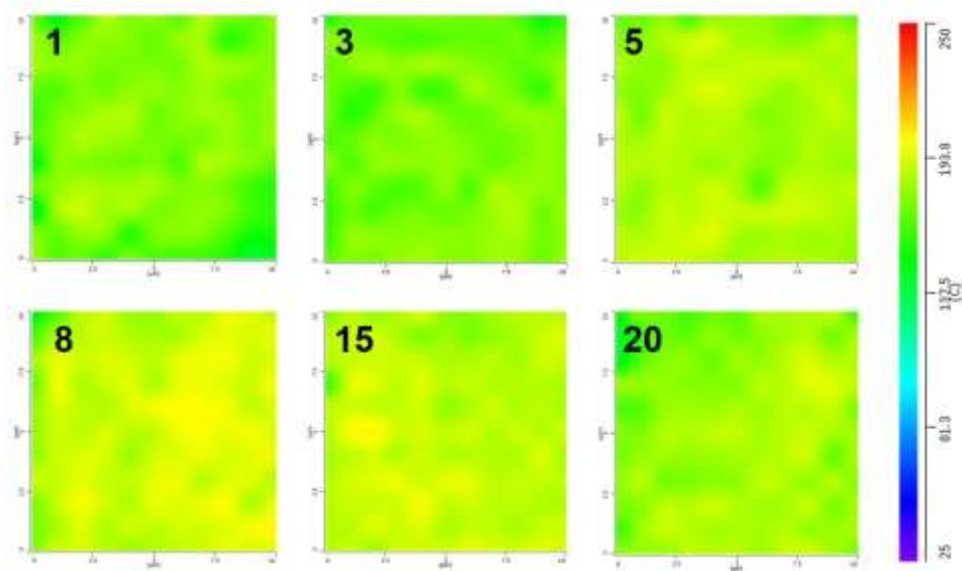
370

371 Figure 4 Transition temperature (n = 100, mean ± SD) and SC protein mass (n = 5,

372 mean ± SD) profiles (A) and their correlation (B) for all 20 tape strips (control study).

373 The number in the plot B represents the tape strip number.

374



375

376 Figure 5 TTM images of the PSC removed from the selected tapes after application of  
377 PG only (area:  $10 \times 10 \mu\text{m}$ ; resolution:  $1 \times 1 \mu\text{m}$ ). The number in the TTM images refers  
378 to the tape strip number.

379

380

381

382

383

384

385

386

387

388

389

390

391 **TABLE:**

392 Table 1 Comparison of transition temperatures for the selected tapes with and without  
393 the application of propylene glycol (PG) (n = 100, mean  $\pm$  SD)

Tape strip no.	Transition temperature ( $^{\circ}$ C)	
	PG	Control
1	175.29 $\pm$ 5.90*	227.76 $\pm$ 5.90
3	174.85 $\pm$ 4.72*	214.89 $\pm$ 5.55
5	184.74 $\pm$ 3.68*	209.60 $\pm$ 5.29
8	191.38 $\pm$ 4.16*	205.55 $\pm$ 2.98
15	188.19 $\pm$ 3.91*	203.54 $\pm$ 2.71
20	181.90 $\pm$ 5.18*	209.98 $\pm$ 2.47

394 \* indicates statistically significant difference (Student's *t* test,  $p < 0.05$ )